Targeting DNA·RNA Hybrids

DOI: 10.1002/anie.200907235

Probing the Molecular Recognition of a DNA·RNA Hybrid Duplex**

Richard T. Wheelhouse, Nichola C. Garbett, Niklaas J. Buurma, and Jonathan B. Chaires*

DNA·RNA hybrid duplexes are the nucleic acid structures least explored as targets in drug discovery. There is a dearth of model ligands displaying convincing structure or sequence selectivity; the secondary structures of the hybrid nucleic acid hosts are variable and complex.[1,2] Ligands selective for hybrid duplexes have potential therapeutic applications as telomerase and RNaseH inhibitors.

Assays for investigating small-molecule interactions with DNA·RNA hybrid duplexes have only recently been developed and described.[3] Herein, their application to the discovery of a small molecule that specifically recognizes poly(dA)·poly(rU) is reported. An unexpected binding mode was uncovered, establishing a principle that extrapolations from pure DNA or RNA binding are invalid when considering DNA·RNA hybrid duplexes.

Competition dialysis (Figure 1) showed that the non-classical intercalator 4,6-bis-[4′-[[2″-(dimethylamino)ethyl]-mercapto]phenyl]pyrimidine dihydrobromide (**1**) bound preferentially to quadruplex and triplex DNA structures and to the hybrid duplex poly(dA)·poly(rU). In duplex binding, strong preferences for both backbone and base orientation were evident: association with the poly(dA)·poly(rU) hybrid duplex had ca. 20-fold preference over the equivalent RNA, 3-fold over DNA, and 7-fold over the alternative poly(rA)·poly(dT) hybrid.

Relative binding preferences for duplex structures were confirmed in a melting of mixtures assay in which UV melting profiles were obtained for a mixture of all four A·T(U) duplexes in the absence and presence of low concentrations of ligand (Figure 2).[3,4] Significant shifting of the melting transition of the poly(dA)·poly(rU) hybrid was accompanied by a lesser shift in the DNA duplex melting curve at higher ligand loading.

CD experiments (Figure 3 a,c) further elucidated the binding interaction. As ligand **1** was titrated into the hybrid solution, the intensity of nucleic acid ellipticity (244 and 275 nm) decreased but the envelope of the spectrum retained its starting shape: indicative of reduced chirality in the oligonucleotide (unwinding) due to intercalation, without alteration of the global conformation. Negative induced CD bands observed for the ligand (320 and 364.5 nm) were also consistent with intercalation.[5] Intercalation was confirmed by a preliminary analytical ultracentrifugation (AUC) experiment in which the sedimentation coefficient decreased upon ligand loading in a manner consistent with unwinding and lengthening of the duplex (see Supporting Information,

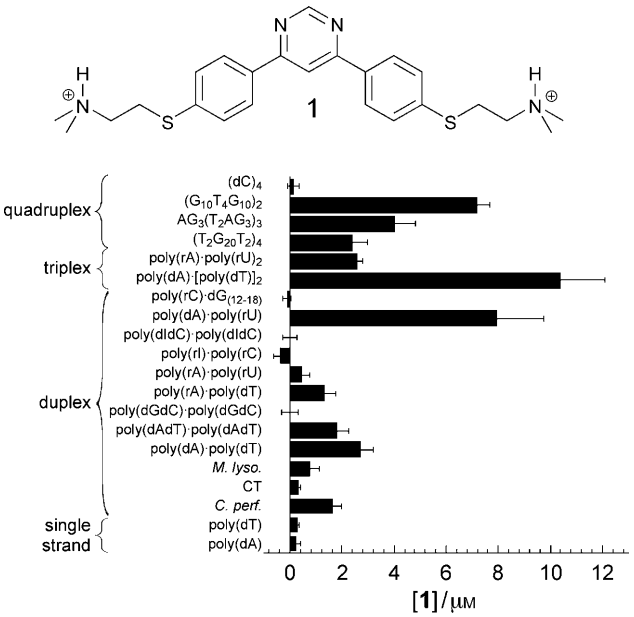

Figure 1. Competition dialysis data for compound **1**. All data are the mean ± standard deviation of three separate determinations.

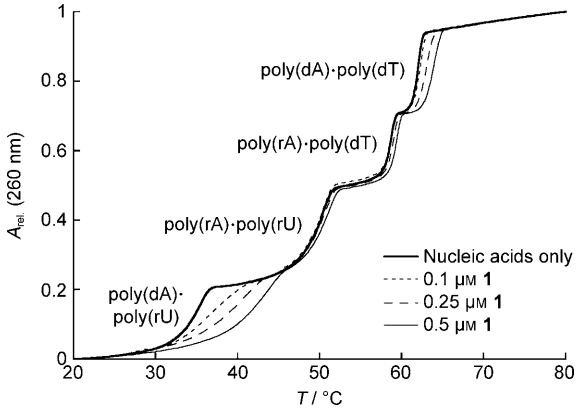

Figure 2. Melting of mixtures data for the four A·T(U) duplexes (each 10 μM(bp)) in the presence of increasing concentrations of ligand **1**.

[*] Dr. R. T. Wheelhouse
School of Pharmacy, University of Bradford
Bradford, BD7 1DP (UK)
E-mail: r.t.wheelhouse@brad.ac.uk
Dr. N. C. Garbett, Prof. J. B. Chaires
James Graham Brown Cancer Center, University of Louisville
Clinical and Translational Research Building
505 S Hancock Street, Louisville, KY 40202 (USA)
Dr. N. J. Buurma
Physical Organic Chemistry Centre
School of Chemistry, Cardiff University
Main Building, Park Place, Cardiff, CF10 3AT (UK)

[**] We thank the British Association for Cancer Research for a Mid-career Fellowship (R.T.W.), the NIH (grant number GM077422; J.B.C.), and the EPSRC (grant number EP/D001641/1; N.J.B.).

Supporting information for this article is available on the WWW under http://dx.doi.org/10.1002/anie.200907235.

 © 2010 Wiley-VCH Verlag GmbH & Co. KGaA, Weinheim

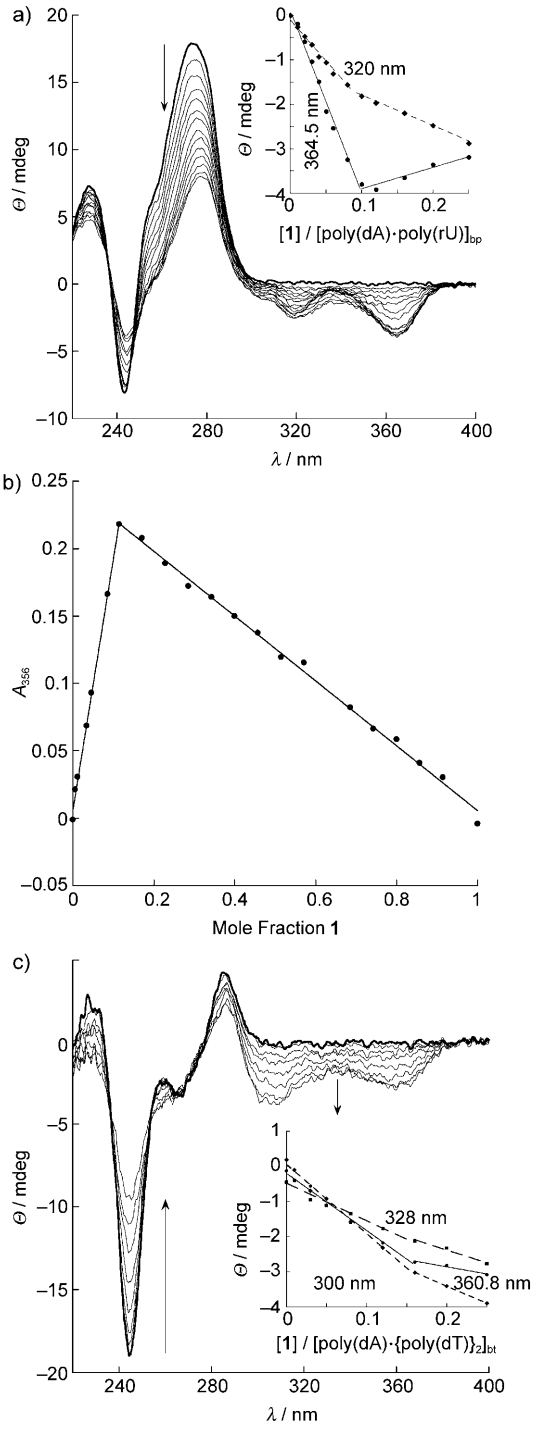

Figure 3. a) CD titration of ligand **1** into poly(dA)·poly(rU) duplex. Inset: induced CD as a function of the [**1**]/[poly(dA)·poly(rU)]$_{bp}$ ratio. b) Job plot for mixtures of compound **1** with poly(dA)·poly(rU) at a constant concentration of 100 μM. c) CD titration of ligand **1** into poly(dA)·[poly(dT)]$_2$ triplex. The spectrum of the free nucleic acid is shown as a bold line. Inset: induced CD as a function of the [**1**]/[poly(dA)·{poly(dT)}$_2$]$_{bt}$ ratio.

Figure S3). Plots of induced CD intensity vs. ligand:base pair ratio (Figure 3a, inset) had an inflection at a ratio of 1:10. The binding stoichiometry of 10 bp per ligand was confirmed by a Job plot (Figure 3b).

CD titration spectra using poly(dA)·[poly(dT)]$_2$ triplex DNA (Figure 3c) reflected those obtained for the hybrid duplex, showing unwinding of the triplex and negative induced CD in the ligand (300, 360.8, 328 nm). The inflection in the induced CD plots (Figure 3c, inset) occurred at a mixing ratio of 0.15, that is, ca. 7 bt per ligand.

Isothermal titration calorimetry (ITC) probed thermodynamic details of the binding interaction. The thermogram for ligand dilution indicated disaggregation of the ligand; data analysis using an isodesmic self-aggregation model yielded $K_{agg} = 4.1 \pm 0.7 \times 10^2\,\text{M}^{-1}$ and $\Delta H_{agg} = -7.3 \pm 0.6\,\text{kcal mol}^{-1}$ (Figures S4, S5). The thermogram for ligand–hybrid interaction indicated (at least) two types of binding site (Figure 4).

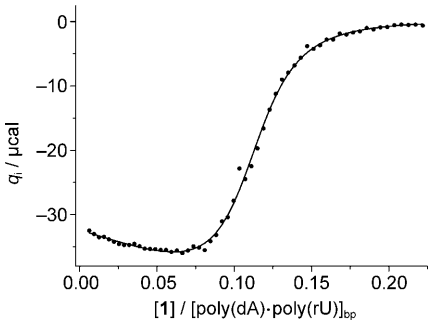

Figure 4. Integrated heat effects for titration of ligand **1** into poly(dA)·poly(rU) fitted using a model involving a major binding site in combination with a minor binding event (see Supporting Information).

ITC data were analyzed using a model describing two consecutive binding events and a model describing two independent binding events; both models incorporated simultaneous ligand self-aggregation (Scheme S1). Strong parameter correlation meant that the two types of site could not be quantified independently in a statistically meaningful way. Nevertheless, analysis of parameter correlation plots concluded that the two binding events are a major binding site of 10 bp in combination with a minor binding event involving ligand association with (potentially fraying) ends and gaps (Supporting Information). The overall binding stoichiometry is consistent with other experimental data for this system and simulated data based on binding parameters from ITC reproduced UV titrations well (Figure S11).

In conclusion, biarylpyrimidine **1** shows a strong preference for binding the poly(dA)·poly(rU) hybrid over all other duplex nucleic acid structures and as a DNA·RNA hybrid binder, inhibited RNaseH[3] with $IC_{50} = 29.5 \pm 0.2$ μM (Figure 5).

All experimental data indicated that each ligand occupied a 10 bp site; CD and AUC data unambiguously showed nucleic acid intercalation. The non-classical intercalator has flexibility of torsion angles between the three aromatic rings. This flexibility may contribute to the binding preference for the A-like hybrid by allowing the ligand to accommodate closely to propeller-twisted base pairs.[6] Ligand **1** also showed binding preferences for triplex and quadruplex nucleic acids. Moreover, triplex poly(dA)·[poly(dT)]$_2$ also exists in an A-like helix. It seems, therefore, that the binding preferences

 © 2010 Wiley-VCH Verlag GmbH & Co. KGaA, Weinheim

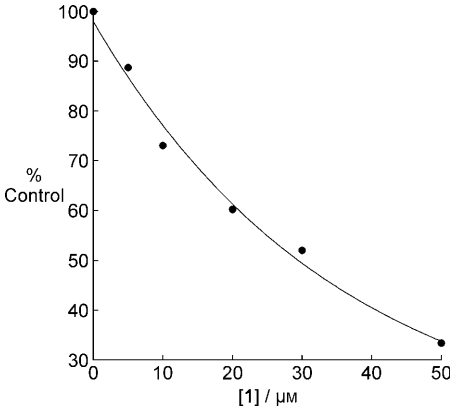

Figure 5. Inhibition of the RNaseH digestion of poly(dA)·poly(rU) by compound **1**; $IC_{50} = 29.5 \pm 0.2$ μM.

discovered are selection for the global A-like structure. In contrast to major groove-binding aminoglycosides,[7] the binding event did not drive a change in the global nucleic acid conformation. Even though the two ligand classes share correlating preferences for triplex structures[8] there was also no evidence that ligand **1** induced hybrid duplex→triplex transitions.

Ligand **1** did not bind to the other A-form structure in Figure 1, the RNA duplex poly(rA)·poly(rU), an observation in contrast to the aminoglycosides, where binding to equivalent RNA duplexes was strong.[7] An explanation may lie in the grooves and the dimensions of the ligand. The ligand possesses two cationic side chains and it may be postulated that one lies in the minor groove. Although the 2′-OH and associated solvation waters of a single RNA strand offer potential hydrogen bonding sites to the terminal ammonium functionality, these groups occlude the minor groove of the pure RNA duplex. Such steric constraints would also account for the reduced affinity of bulkier analogs of ligand **1** for the hybrid duplex (Figure S12). Indeed the hybrid minor groove appears inaccessible to all but the smallest groups: pentamidine, berenil, Hoechst 33258, and DAPI (4′,6-diamidino-2-phenylindole) all failed to stabilize either of the hybrid duplexes in the melting of mixtures assay.[3]

Binding rules for DNA·RNA duplexes are ill-defined, and this study shows that naive extrapolation from duplex binding models is inappropriate. The structural basis for the ca. 10 bp major binding site size is not yet clear but is equivalent to ca. 1 ligand per helical turn. The intercalator ethidium has been shown to exclude 3 or 7 bp when bound to the poly(dA)·poly(rU) hybrid,[9,10] and precedent for long-range transmission of binding effects over tens to hundreds of bp exists in the daunorubicin-driven Z→B conversion of $[poly(dGdC)]_2$.[11]

DNA·RNA hybrids and DNA triplexes both adopt structures intermediate between classic B-form DNA and A-form RNA. The correlation between binding data for ligand **1** and its analogs to these two structures is striking (Figures 3 and S13) and demonstrates that the search for structure and sequence-selective ligands for DNA·RNA hybrid duplexes should start with re-evaluation of DNA triplex-targeting compounds.

Experimental Section

Compound **1** was synthesized as previously described.[12,13] Oligonucleotides for CD and calorimetry were obtained from Midland Certified Reagent Co, Midland, TX (poly(dA), lot 111997, 126–1200 nucleotides; poly(rU) lot 102197, 500–2600 nucleotides). All other oligonucleotides were purchased from Sigma, Milwaukee, WI, USA or Poole, UK.

CD spectra were recorded on a Jasco J-810 spectropolarimeter with a Peltier temperature controller. UV melting experiments were performed on a Cary 400Bio spectrophotometer equipped with a Peltier temperature controller. Other spectra were recorded on a Jasco V-550 spectrophotometer and Tecan Safire^2 microplate reader. ITC was performed on a Microcal VP-ITC calorimeter.

Competition dialysis,[3,14–17] melting of mixtures[3,4] and RNaseH assays[3,4] followed published protocols.

Job plots: The protocol followed that set out by Jenkins[18] but using UV detection. Mixtures of **1** and poly(dA)·poly(rU) to a summed concentration of 100 μM in BPES pH 6.00 (BPES: buffer phosphate EDTA sodium) were set up in duplicate on a 96-well microtiter plate. Reference solutions contained buffer in place of nucleic acid. Spectra were recorded in the 230 to 450 nm range. Data for the ligand absorbance maximum at 356 nm were extracted and the free ligand absorbance subtracted from that of the drug–nucleic acid complex before plotting A_{356} vs. mole fraction of ligand.

CD Titrations: Nucleic acid solutions in BPES pH 6.00 (1 mL) were prepared to have $A_{257} \approx 0.8$ and placed in a 1 cm pathlength quartz cuvette equipped with stirrer. Concentrated ligand solutions were prepared in the same buffer to minimize volume changes during titration. Aliquots were added until precipitation of the ligand–nucleic acid complex was evident. Raw data were corrected for dilution before plotting and analysis.

ITC: all experiments were performed in BPES pH 6.00. Oligonucleotides were dissolved in buffer, dialyzed against buffer (3 changes of solution) and the final dialysate used as solvent for all experiments and dilution of reagents. In a typical experiment, a solution of poly(dA)·poly(rU) (0.5 mM(bp)) was loaded into the calorimeter cell and ligand **1** (0.25 mM) loaded into the syringe; aliquots (10 μL) were added at intervals of 360 s. To determine the heats of dilution, a solution of **1** (5 mM) was titrated (15 μL aliquots, 360 s) into buffer. Other control titrations of buffer into nucleic acid and buffer into buffer were also performed. Data were treated in Origin (Microcal, Inc) to generate integrated heat effects per injection (Δh). These were analyzed using IC ITC following published procedures.[19,20] Ligand self-aggregation parameters were determined from ligand dilution experiments and held constant in subsequent analyses of binding data.

Received: December 22, 2009
Published online: March 29, 2010

Keywords: DNA–RNA hybrids · drug discovery · molecular recognition · pyrimidine · RNaseH

[1] N. N. Shaw, D. P. Arya, *Biochimie* **2008**, *90*, 1026.
[2] J. I. Gyi, G. L. Conn, A. N. Lane, T. Brown, *Biochemistry* **1996**, *35*, 12538.
[3] R. T. Wheelhouse, J. B. Chaires in *Drug-DNA Interaction Protocols*, 2nd ed. (Ed.: K. R. Fox), Springer, Heidelberg, **2010**.
[4] X. C. Shi, J. B. Chaires, *Nucleic Acids Res.* **2006**, *34*, e14.
[5] N. C. Garbett, P. A. Ragazzon, J. B. Chaires, *Nat. Protoc.* **2007**, *2*, 3166.
[6] W. D. Wilson, F. A. Tanious, R. A. Watson, H. J. Barton, A. Strekowska, D. W. Boykin, L. Strekowski, *Biochemistry* **1989**, *28*, 1984.

 © 2010 Wiley-VCH Verlag GmbH & Co. KGaA, Weinheim

[7] C. M. Barbieri, T. K. Li, S. Guo, G. Wang, A. J. Shallop, W. Pan, G. Yang, B. L. Gaffney, R. A. Jones, D. S. Pilch, *J. Am. Chem. Soc.* **2003**, *125*, 6469.
[8] D. P. Arya, R. L. Coffee, Jr., I. Charles, *J. Am. Chem. Soc.* **2001**, *123*, 11093.
[9] E. A. Lehrman, D. M. Crothers, *Nucleic Acids Res.* **1977**, *4*, 1381.
[10] N. N. Shaw, H. Xi, D. P. Arya, *Bioorg. Med. Chem. Lett.* **2008**, *18*, 4142.
[11] X. Qu, J. O. Trent, I. Fokt, W. Priebe, J. B. Chaires, *Proc. Natl. Acad. Sci. USA* **2000**, *97*, 12032.
[12] R. T. Wheelhouse, S. A. Jennings, V. A. Phillips, D. Pletsas, P. M. Murphy, N. C. Garbett, J. B. Chaires, T. C. Jenkins, *J. Med. Chem.* **2006**, *49*, 5187.
[13] P. M. Murphy, V. A. Phillips, S. A. Jennings, N. C. Garbett, J. B. Chaires, T. C. Jenkins, R. T. Wheelhouse, *Chem. Commun.* **2003**, 1160.
[14] J. S. Ren, J. B. Chaires, *Biochemistry* **1999**, *38*, 16067.
[15] J. S. Ren, J. B. Chaires, *J. Am. Chem. Soc.* **2000**, *122*, 424.
[16] J. S. Ren, J. B. Chaires, *Methods Enzymol.* **2001**, *340*, 99.
[17] J. B. Chaires, *Curr. Med. Chem. Anti-Cancer Agents* **2005**, *5*, 339.
[18] T. C. Jenkins in *Drug-DNA Interaction Protocols* (Ed.: K. R. Fox), Humana, Totowa, USA, **1997**, p. 195.
[19] N. J. Buurma, I. Haq, *J. Mol. Biol.* **2008**, *381*, 607.
[20] N. J. Buurma, I. Haq, *Methods* **2007**, *42*, 162.

 © 2010 Wiley-VCH Verlag GmbH & Co. KGaA, Weinheim